

OPTICAL FIBRES AND FIBRE AMPLIFIERS

PACS numbers: 42.81.Dp; 42.79.Dj
DOI: 10.1070/QE2012v042n03ABEH014786

Bragg fibres with an intermediate layer

Yu.N. Kulchin, Yu.A. Zinin, I.G. Nagorny

Abstract. **This paper examines the effect of an intermediate layer between the core and periodic cladding of a Bragg fibre on its optical properties. It is shown that any TE_{0k} mode of a standard Bragg fibre can be transformed into the fundamental mode of a Bragg fibre with an intermediate layer by adjusting the thickness of the first cladding layer. Varying the thickness of the intermediate layer, one can tune the mode composition of the transmitted light in a periodic manner. The periodic variation of the optical loss with the thickness of the intermediate layer is due to resonances and antiresonances in this layer. The resonances correspond to two-mode light propagation through the fibre, whereas the antiresonances, to single-mode light propagation.**

Keywords: *optical characteristics of fibres, Bragg fibres.*

1. Introduction

Bragg fibres are multilayer waveguides widely used in optics. Their optical properties are governed by Fresnel reflection from the interfaces in the multilayer periodic structure of their cladding, whereas the optical properties of conventional fibres are governed by total internal reflection from the surface of the denser core. For this reason, even hollow-core Bragg fibres can have rather low optical losses [1, 2], low bend sensitivity [3], large mode area [4] and a number of other unique properties.

The properties of Bragg fibres have been the subject of extensive studies (see, e.g. Refs [5–10]), most of which were concerned with fibres consisting of a core and a periodic layered cladding around the core. Mizrahi and Schachter [11] considered a fibre with a matching layer of a certain thickness between a hollow core and periodic cladding and analysed the effect of the matching layer on the zero-dispersion region of the fibre and the mode field distribution in its core. The thickness of the intermediate layer was chosen so as to maximise internal reflection at the interface between the intermediate layer and the first layer of the periodic cladding.

This paper examines the effect of parameters of an intermediate layer on the mode composition of propagating light and the optical loss in the fibre.

Yu.N. Kulchin, Ya.A. Zinin Institute for Automation and Control Processes, Far Eastern Branch, Russian Academy of Sciences, ul. Radio 5, 690041 Vladivostok, Russia;
I.G. Nagorny Far Eastern Federal University, ul. Sukhanova 8, 690000 Vladivostok, Russia; e-mail: ngrn@iacp.phys.dvo.ru

Received 2 December 2011; revision received 20 January 2012
Kvantovaya Elektronika **42** (3) 235–240 (2012)
Translated by O.M. Tsarev

2. Dispersion equation

To assess the optical characteristics of a Bragg fibre with an intermediate layer, we use the transfer matrix method. The mathematical framework for this method has been described in several publications (see, e.g. Refs [12–15]).

For an arbitrary homogeneous cylindrical layer, the axial and azimuthal components of the electromagnetic field (E_z, E_ϕ, H_z, and H_ϕ) can be expressed through a linear combination of two cylindrical functions: Bessel functions of the first and second kinds [5], Hankel functions of the first and second kinds [12] and Bessel and Hankel functions of the first kind [13]. At an arbitrary azimuthal mode number, m, a pair of Bessel functions of the first and second kinds and a pair of Hankel functions of the first and second kinds (all of order m) are a fundamental system of solutions to the Bessel differential equation [16]. Using a combination of Bessel functions of the first and second kinds, one can determine the mode composition of light propagating through a fibre, but an additional algorithm is needed to calculate the optical loss [10].

For this reason, we use a combination of Hankel functions of the first and second kinds: $H_m^{(1)}(kr)$ and $H_m^{(2)}(kr)$. The electromagnetic field components in the jth layer can be represented as follows [where the $\exp(i\beta z)$ factor, common to all the field components, is omitted]:

$$
\begin{aligned}
E_z &= [A_j H_m^{(1)}(k_j r) + B_j H_m^{(2)}(k_j r)] \begin{Bmatrix} \cos m\phi \\ \sin m\phi \end{Bmatrix}, \\
E_\phi &= \frac{i\beta m}{r k_j^2} [A_j H_m^{(1)}(k_j r) + B_j H_m^{(2)}(k_j r)] \begin{Bmatrix} \sin m\phi \\ -\cos m\phi \end{Bmatrix} \\
&\quad + \frac{i\omega\mu}{c k_j} [C_j \dot{H}_m^{(1)}(k_j r) + D_j \dot{H}_m^{(2)}(k_j r)] \begin{Bmatrix} \sin m\phi \\ \cos m\phi \end{Bmatrix}, \\
H_z &= [C_j H_m^{(1)}(k_j r) + D_j H_m^{(2)}(k_j r)] \begin{Bmatrix} \sin m\phi \\ \cos m\phi \end{Bmatrix}, \qquad (1) \\
H_\phi &= -\frac{i\omega\varepsilon}{c k_j} [A_j \dot{H}_m^{(1)}(k_j r) + B_j \dot{H}_m^{(2)}(k_j r)] \begin{Bmatrix} \cos m\phi \\ \sin m\phi \end{Bmatrix} \\
&\quad - \frac{i\beta m}{r k_j^2} [C_j H_m^{(1)}(k_j r) + D_j H_m^{(2)}(k_j r)] \begin{Bmatrix} \cos m\phi \\ -\sin m\phi \end{Bmatrix},
\end{aligned}
$$

where n_j and k_j are the refractive index of and the transverse wave vector component in the jth layer; $k_j^2 = k_0^2(n_j^2 - \beta^2/k_0^2)$; k_0 is the wave vector in vacuum; μ is the magnetic permeability of the medium; β is the propagation constant of the guided mode; $\beta/k_0 = n_{\text{eff}}$ is its effective refractive index; and A_j, B_j, C_j,

and D_j are the amplitude constants of the electromagnetic field components in the jth layer.

The longitudinal electromagnetic field components must be continuous across the boundaries of the layers. The boundary conditions can be written in matrix form:

$$\begin{pmatrix} A_{j+1} \\ B_{j+1} \\ C_{j+1} \\ D_{j+1} \end{pmatrix} = M(r_j) \begin{pmatrix} A_j \\ B_j \\ C_j \\ D_j \end{pmatrix}, \tag{2}$$

where $M(r_j)$ is a 4×4 matrix consisting of elements m_{gq} (g is the number of the line and q is the number of the column).

The matrix elements have the form

$$m_{11} = 0.25\mathrm{i}\pi y_j \left\{ H_m^{(1)}(x_j)\dot{H}_m^{(2)}(y_j) - \frac{\varepsilon_j y_j}{\varepsilon_{j+1} x_j} \dot{H}_m^{(1)}(x_j) H_m^{(2)}(y_j) \right\},$$

$$m_{12} = 0.25\mathrm{i}\pi y_j \left\{ H_m^{(2)}(x_j)\dot{H}_m^{(2)}(y_j) - \frac{\varepsilon_j y_j}{\varepsilon_{j+1} x_j} \dot{H}_m^{(2)}(x_j) H_m^{(2)}(y_j) \right\},$$

$$m_{13} = \frac{0.125\mathrm{i} y_j m\beta\lambda_0}{\varepsilon_{j+1}} \left\{ \frac{1}{y_j} - \frac{y_j}{x_j^2} \right\} H_m^{(1)}(x_j) H_m^{(2)}(y_j),$$

$$m_{14} = \frac{0.125\mathrm{i} y_j m\beta\lambda_0}{\varepsilon_{j+1}} \left\{ \frac{1}{y_j} - \frac{y_j}{x_j^2} \right\} H_m^{(2)}(x_j) H_m^{(2)}(y_j),$$

$$m_{21} = 0.25\mathrm{i}\pi y_j \left\{ \frac{\varepsilon_j y_j}{\varepsilon_{j+1} x_j} \dot{H}_m^{(1)}(x_j) H_m^{(1)}(y_j) - H_m^{(1)}(x_j)\dot{H}_m^{(1)}(y_j) \right\},$$

$$m_{22} = 0.25\mathrm{i}\pi y_j \left\{ \frac{\varepsilon_j y_j}{\varepsilon_{j+1} x_j} \dot{H}_m^{(2)}(x_j) H_m^{(1)}(y_j) - H_m^{(2)}(x_j)\dot{H}_m^{(1)}(y_j) \right\},$$

$$m_{23} = \frac{0.125\mathrm{i} y_j m\beta\lambda_0}{\varepsilon_{j+1}} \left\{ \frac{y_j}{x_j^2} - \frac{1}{y_j} \right\} H_m^{(1)}(x_j) H_m^{(1)}(y_j),$$

$$m_{24} = \frac{0.125\mathrm{i} y_j m\beta\lambda_0}{\varepsilon_{j+1}} \left\{ \frac{y_j}{x_j^2} - \frac{1}{y_j} \right\} H_m^{(2)}(x_j) H_m^{(1)}(y_j),$$

$$m_{31} = 0.125\mathrm{i} y_j m\beta\lambda_0 \left\{ \frac{1}{y_j} - \frac{y_j}{x_j^2} \right\} H_m^{(1)}(x_j) H_m^{(2)}(y_j),$$

$$m_{32} = 0.125\mathrm{i} y_j m\beta\lambda_0 \left\{ \frac{1}{y_j} - \frac{y_j}{x_j^2} \right\} H_m^{(2)}(x_j) H_m^{(2)}(y_j),$$

$$m_{33} = 0.25\mathrm{i}\pi y_j \left\{ H_m^{(1)}(x_j)\dot{H}_m^{(2)}(y_j) - \frac{y_j}{x_j} \dot{H}_m^{(1)}(x_j) H_m^{(2)}(y_j) \right\},$$

$$m_{34} = 0.25\mathrm{i}\pi y_j \left\{ H_m^{(2)}(x_j)\dot{H}_m^{(2)}(y_j) - \frac{y_j}{x_j} \dot{H}_m^{(2)}(x_j) H_m^{(2)}(y_j) \right\},$$

$$m_{41} = 0.125\mathrm{i} y_j m\beta\lambda_0 \left\{ \frac{y_j}{x_j^2} - \frac{1}{y_j} \right\} H_m^{(1)}(x_j) H_m^{(1)}(y_j),$$

$$m_{42} = 0.125\mathrm{i} y_j m\beta\lambda_0 \left\{ \frac{y_j}{x_j^2} - \frac{1}{y_j} \right\} H_m^{(2)}(x_j) H_m^{(1)}(y_j),$$

$$m_{43} = 0.25\mathrm{i}\pi y_j \left\{ \frac{y_j}{x_j} \dot{H}_m^{(1)}(x_j) H_m^{(1)}(y_j) - H_m^{(1)}(x_j)\dot{H}_m^{(1)}(y_j) \right\},$$

$$m_{44} = 0.25\mathrm{i}\pi y_j \left\{ \frac{y_j}{x_j} \dot{H}_m^{(2)}(x_j) H_m^{(1)}(y_j) - H_m^{(2)}(x_j)\dot{H}_m^{(1)}(y_j) \right\}, \tag{3}$$

where $x_j = k_j r_j$; $y_j = k_{j+1} r_j$; λ_0 is the wavelength in vacuum; and ε_j is the relative dielectric permittivity of the jth layer.

The constants A, B, C and D for the $(j+1)$th layer of the cladding are related to those for the core by

$$\begin{pmatrix} A_{j+1} \\ B_{j+1} \\ C_{j+1} \\ D_{j+1} \end{pmatrix} = \prod_{i+1}^{j} M(r_i) \begin{pmatrix} A_1 \\ B_1 \\ C_1 \\ D_1 \end{pmatrix}. \tag{4}$$

Outside the fibre, there should be no reflected wave, so the constants B_{N+1} and D_{N+1} for a fibre having N layers are zero. A solution to Eqn (4) at $j = N$ exists provided that

$$(p_{23} + p_{24})(p_{41} + p_{42}) - (p_{43} + p_{44})(p_{21} + p_{22}) = 0, \tag{5}$$

where p_{gq} are the elements of the matrix obtained by multiplying all the $M(r_i)$ matrices. Equation (5) can be used to find the modes of a multilayer cylindrical fibre.

Equation (5) takes a simpler form when the azimuthal mode number is zero. In the case of $TM_{0\kappa}$ modes, where κ is the radial mode number, we obtain

$$p_{21} + p_{22} = 0, \tag{6}$$

In the case of $TE_{0\kappa}$ modes, we have

$$p_{43} + p_{44} = 0. \tag{7}$$

The optical loss, γ, is defined as a reduction in the intensity of light propagating through the fibre: $\gamma = (4\pi \mathrm{Im}\, n_{\mathrm{eff}})/\lambda_0$, or (in dB m^{-1})

$$\gamma = \frac{40\pi \lg \mathrm{e}}{\lambda_0} \mathrm{Im}\, n_{\mathrm{eff}}. \tag{8}$$

At a given fibre geometry, each of the dispersion relations (5)–(7) has several possible solutions, which define a set of complex values of n_{eff}. The different $\mathrm{Re}\, n_{\mathrm{eff}}$ values will be referred to as roots of the dispersion equation. When a fibre parameter is varied continuously, the roots also vary continuously. A continuous dependence of any physical quantity on a fibre parameter for each root will be referred to as a root curve. Changes in $\mathrm{Re}\, n_{\mathrm{eff}}$ are accompanied by changes in $\mathrm{Im}\, n_{\mathrm{eff}}$ and, hence, in the optical loss in the fibre and its transmission.

3. Modes of Bragg fibres with an intermediate layer

Figure 1 shows the radial refractive index profile of a Bragg fibre with an intermediate layer. In contrast to that in conventional Bragg fibres, the layer adjacent to the core differs from the other layers in the periodic cladding. As an example, let us consider the fibre described by Bassett and Argyros [2] and vary the thickness of the layer adjacent to the core. Because this layer differs from those in the periodic cladding, it will be referred to as an intermediate layer.

Calculations were performed for a Bragg fibre having a hollow core of radius r_1 and a matching layer of thickness d_{M} with a refractive index $n_{\mathrm{M}} = 1.49$. The periodic cladding consists of alternating layers of thickness $d_{\mathrm{L}} = 0.346$ μm and $d_{\mathrm{H}} = 0.2133$ μm with refractive indices n_{L}=1.17 and n_{H}=1.49. The number of layers around the core is $N = 32$.

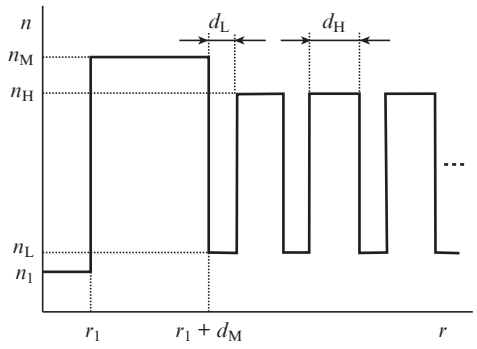

Figure 1. Schematic of a Bragg fibre with an intermediate layer.

Fibres with $d_M = d_H = 0.2133$ μm and $r_1 = 1.3278$ (fibre A) or 1.8278 μm (fibre B) were examined in a number of studies [2, 9, 10, 13]. Such a fibre geometry is nearly optimal for 1-μm light, and the cladding layers are almost quarter-wave thick [13].

Table 1 lists all possible solutions to Eqn (7) and the corresponding optical losses [see Eqn (8)] for fibre B, as well as the roots of the dispersion equation, numbered in the order of decreasing $\mathrm{Re}\, n_{\mathrm{eff}}$.

Table 1. Roots of the dispersion equation for a Bragg fibre having 32 layers in a periodic cladding with $d_H = 0.2133$ mm, $d_L = 0.346$ μm, $n_H = 1.49$ and $n_L = 1.17$. The radius of the hollow core is $r_1 = 1.8278$ μm, and the wavelength is $\lambda_0 = 1$ μm..

$\mathrm{Re}\, n_{\mathrm{eff}}$	$\mathrm{Im}\, n_{\mathrm{eff}}$	γ/dB m^{-1}	m	κ	Root
0.94176190	0.92087314E-09	5.0257E-02	0	1	1
0.81268486	0.31488555E-04	1718.4896	0	2	2
0.78912478	0.22799474E-02	124428.2529	0	2	3
0.75371929	0.66313973E-02	361908.8668	0	3	4
0.70293911	0.12067946E-01	658608.8066	0	3	5
0.63952600	0.17781726E-01	970438.6596	0	3	6
0.56736635	0.22547231E-01	1230516.3531	0	3	7
0.48838666	0.29939431E-01	1633946.0685	0	3	8
0.38222431	0.50127307E-01	2735700.4947	0	4	9
0.21542752	0.10916140E+00	5957489.3178	0	4	10

The radial mode number κ is determined by the field distribution across the fibre core. The radial electric and magnetic field distributions are proportional to the Bessel function $J_1(k_1 r)$ [14], where k_1 is the transverse wave vector component in the core. The value of κ is also determined by the $k_1 r$ product. At $r = 0$, we have $J_1(k_1 r) = 0$.

The procedure for finding the κ of a conventional optical fibre can be used to find the radial mode number in a Bragg fibre. The magnitude of κ is here uniquely determined by the field distribution across the fibre core. We have $\kappa = 1$ in the range $0 < k_1 r < 2.405$, $\kappa = 2$ in the range $2.405 \leqslant k_1 r < 3.83$, etc. At $r_1 = 1.8278$ μm, $\kappa = 1$ corresponds to $\mathrm{Re}\, n_{\mathrm{eff}}$ from 0.9427 to 1.0; $\kappa = 2$, to the range 0.7917–0.9427; $\kappa = 3$, to 0.4640–0.7917; and $\kappa = 4$, to 0–0.4640.

Note that this procedure is inadequate for determining modes of a Bragg fibre, because these result from interference of the light reflected from different cladding layers.

The arguments of modes with low optical losses at the core–cladding interface ($r = r_1$) correspond to nearly zero values of the Bessel function $J_1(k_1 r_1)$. The mode on the topmost line in Table 1 has $\mathrm{Re}\, n_{\mathrm{eff}} = 0.9417619$, which is only slightly less than the $\mathrm{Re}\, n_{\mathrm{eff}} = 0.942699$ corresponding to the second zero of $J_1(k_1 r_1)$. Nevertheless, this mode is thought of as TE_{01} [2, 9, 10, 13]. Modes with significant optical losses may have $k_1 r_1$ values far away from the zeros of the Bessel function.

Below, we use a simplified procedure for determining the radial mode number in a Bragg fibre. To this end, we shift the lower limit of $\mathrm{Re}\, n_{\mathrm{eff}}$ for each mode, evaluated from the radial distribution, by 1/100 of the range of effective refractive indices of the $(\kappa + 1)$th mode, evaluated from the zeros of $J_1(k_1 r_1)$. Since the magnitude of the down correction is unimportant for further analysis, the shift by 1% is not exact and is only used for an arbitrary estimate. Given this, the lower limit of $\mathrm{Re}\, n_{\mathrm{eff}}$ for the first κ's is 0.941198 and 0.787445, and that for $\kappa = 3$ is 0.45933.

It follows from Table 1 that there are five TE_{03} modes and two TE_{04} modes, which differ in the angle between the beam and fibre axis. The optical loss of these modes is very high, and they are left out of consideration in the case of standard Bragg fibres. Since the optical loss of any transverse or hybrid mode far exceeds that of the TE_{01} mode, the latter is the fundamental mode of the fibre under consideration.

Figure 2a shows $\mathrm{Re}\, n_{\mathrm{eff}}$ (the first two roots) as a function of hollow core radius, r_1, for the TE_{01} and TE_{02} modes of a fibre with a periodic structure [2]. With increasing r_1, $\mathrm{Re}\, n_{\mathrm{eff}}$ increases, approaching unity. The $\mathrm{Re}\, n_{\mathrm{eff}}$ of the latter mode is always smaller than that of the former mode. The optical loss decreases with increasing r_1 (Fig. 2b) for both modes, and the optical loss of the latter mode is only a few times higher than that in the former. For example, at $r_1 = 9.0$ μm, the n_{eff}'s of the first three modes are 0.99767557 + i0.94900016E−11,

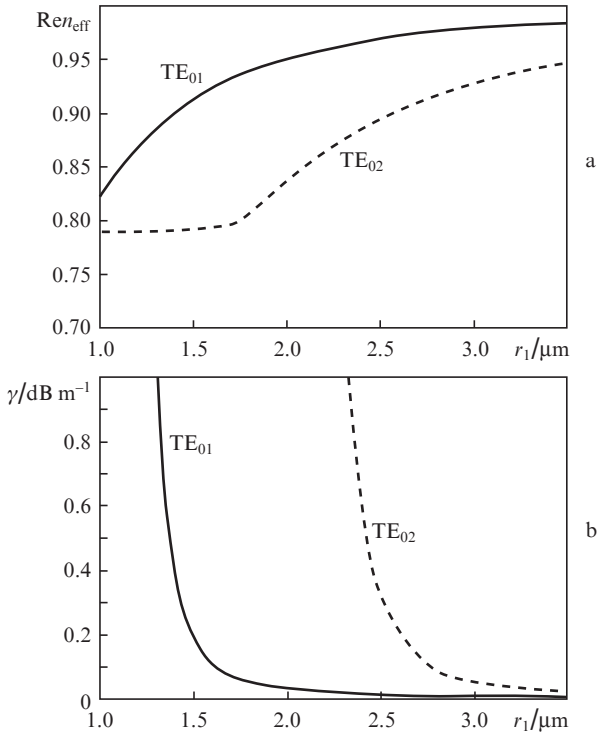

Figure 2. (a) Effective refractive index and (b) optical loss as functions of hollow core radius for the TE_{01} and TE_{02} modes of a Bragg fibre. The periodic cladding is composed of 32 layers of thickness $d_H = 0.2133$ μm and $d_L = 0.346$ μm with refractive indices $n_H = 1.49$ and $n_L = 1.17$; $\lambda_0 = 1$ μm.

0.99219255 + i0.27438443E−10 and 0.98353542 + i0.48744394E−10.

The behaviour of $\mathrm{Re}\,n_{\mathrm{eff}}$ depends significantly on the thickness of the layer adjacent to the core. $\mathrm{Re}\,n_{\mathrm{eff}}$ can reach the refractive index of the core and even slightly exceed it. In the latter case, TE_{01} becomes a cladding mode, its optical loss increases sharply, and it disappears.

The corresponding root is then no longer a solution to the dispersion equation, and the next root becomes the solution with the highest $\mathrm{Re}\,n_{\mathrm{eff}}$ value.

Figure 3b shows the optical loss as a function of matching-layer thickness for the first five roots. The first root curve has the lowest optical loss at a matching-layer thickness of 0.259 μm. At higher d_{M} values, the optical loss increases as long as this root is a solution to Eqn (7). In the second curve (corresponding to the second root in Table 1), the optical loss first decreases with increasing d_{M} and is equal to that in the first root curve at $d_{\mathrm{M}} = 0.485$ μm (point C). A fibre with such a geometry will have the highest loss and support two modes (the first root curve in this region corresponds to the TE_{01} mode, and the second, to the TE_{02} mode). With a further increase in d_{M}, the optical loss in the second root curve continues to decrease, differing by orders of magnitude from that in the other root curves, and the fibre again supports only one mode.

The optical loss in the second root curve has a minimum near $d_{\mathrm{M}} = 0.6936$ (point D) and then increases, intersecting the decreasing optical loss in the third root curve (point E), and the above situation repeats itself.

Thus, increasing the thickness of the matching layer leads to a continuous increase in $\mathrm{Re}\,n_{\mathrm{eff}}$ for each root in Table 1, changing the azimuthal mode number, κ, because the core radius remains constant. The root curve will correspond not to a particular mode with fixed κ and $m = 0$, but different portions of the root curve will correspond to different modes with $m = 0$ and different κ values. The horizontal lines in Fig. 3a represent tentative boundaries where κ changes by unity. Changing the correction used to determine modes will slightly shift the boundaries, but the root curve will nevertheless intersect them.

Thus, the root curve corresponds to a tunable mode with various radial mode numbers. Any $TE_{0\kappa}$ mode of a standard Bragg fibre can be tuned to give the fundamental mode of a Bragg fibre with an intermediate layer by varying the thickness of the first cladding layer.

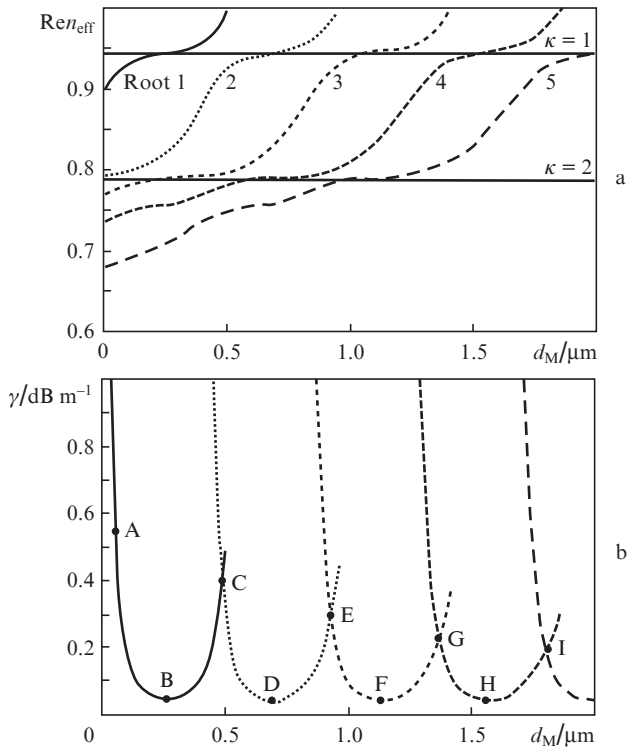

Figure 3. (a) Effective refractive index and (b) optical loss against the thickness of the first cladding layer ($n_{\mathrm{M}} = 1.49$), adjacent to the core, for roots 1–5 of the dispersion equation (see Table 1). The radius of the hollow core is $r_1 = 1.8278$ μm, and the wavelength is $\lambda_0 = 1$ μm. The periodic cladding is composed of 31 layers of thickness $d_{\mathrm{L}} = 0.346$ μm and $d_{\mathrm{H}} = 0.2133$ μm with refractive indices $n_{\mathrm{L}} = 1.17$ and $n_{\mathrm{H}} = 1.49$. The horizontal lines in Fig. 3a represent tentative boundaries of the radial mode numbers.

4. Optical loss in Bragg fibres with an intermediate layer

The optical loss in a standard Bragg fibre with almost quarter-wave thick cladding layers is dominated by the optical loss of the fundamental mode because the absorption coefficients of the other modes are considerably greater and light can be thought to propagate in single-mode fashion. The optical loss in a Bragg fibre with an intermediate layer and almost quarter-wave thick periodic cladding layers is determined by the minimal optical loss of the corresponding mode at a given fibre geometry (for example, the composite curve ABCDEFGHI in Fig. 3b). This approximation will be quite accurate in the single-mode and quasi-single-mode ranges. In the two-mode ranges, which can be thought of as narrow (the derivatives of the intersecting curves for the competing modes TE_{01} and TE_{02} are opposite in sign in the vicinity of points C, E, G and I), the resultant curve ABCDEFGHI is distorted only slightly. The optical loss calculated for $TM_{0\kappa}$ transverse modes using Eqns (6) and (8) is several orders of magnitude higher than that corresponding to the resultant curve for any thickness of the intermediate layer. Because the optical loss calculated for the other transverse and any hybrid modes ($1 \leqslant m \leqslant 7$) using Eqns (5) and (8) considerably exceeds that corresponding to the ABCDEFGHI curve, we will think this curve to represent the optical loss of the Bragg fibre under consideration. For higher order modes ($m > 7$), we did not calculate the optical loss as a function of intermediate-layer thickness for each root because such calculations would require considerable effort. Calculation results for a number of modes with $m > 7$ at a constant thickness of the intermediate layer demonstrate that the optical loss increases with increasing m.

Figure 4 shows the optical loss γ as a function of $\mathrm{Re}\,n_{\mathrm{eff}}$ at two values of r_1. Curves (*1*) were constructed in the vicinity of point B (see Fig. 3b); curves (*2*), in the vicinity of point D; etc. It is seen that the optical loss is lowest in a certain $\mathrm{Re}\,n_{\mathrm{eff}}$ range. Each root curve lies in the transmission window at a certain thickness of the intermediate layer. The greater the number of the root curve, the thicker the intermediate layer.

Since n_{eff} is proportional to β, varying the thickness of the intermediate layer one can control the field distribution in the core and the wave vector direction. The range of angles will be determined by the range of $\mathrm{Re}\,n_{\mathrm{eff}}$ values corresponding to the minimum optical loss for a particular root curve.

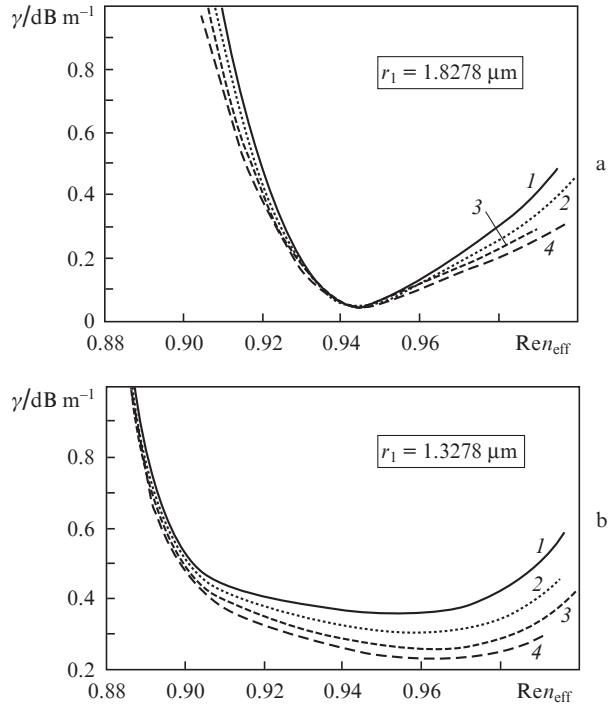

Figure 4. Minimal optical loss as a function of effective refractive index at different values of r_1. The numbers of the curves correspond to the numbers of the roots of the dispersion equation. In Fig. 4a, curve (*1*) was constructed in the vicinity of point B (see Fig. 3b); curve (*2*), in the vicinity of point D; etc. The parameters of the periodic cladding are the same as in Fig. 3; $\lambda_0 = 1$ μm.

The $\mathrm{Re}\,n_{\mathrm{eff}}(d_{\mathrm{M}})$ curves in Fig. 5, obtained for different core radii, r_1, illustrate the behaviour of $\mathrm{Re}\,n_{\mathrm{eff}}$ for the lowest loss root curves. In the two-mode range, we took $\mathrm{Re}\,n_{\mathrm{eff}}$ for the lowest loss root curve. Sharp changes in $\mathrm{Re}\,n_{\mathrm{eff}}$ correspond to a situation where a mode of another root curve becomes the lowest loss mode. For illustrative purposes, we connected branches of different root curves corresponding to a given r_1 value. Even though the vertical portions of the curves in Fig. 5 do not represent the behaviour of $\mathrm{Re}\,n_{\mathrm{eff}}$ for any actual fibre modes, they can be used to estimate the range in which the effective refractive index varies.

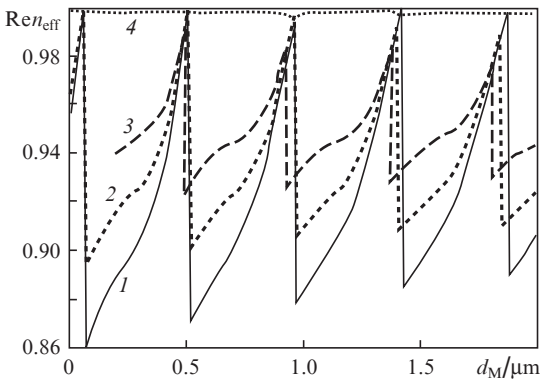

Figure 5. Effective refractive index as a function of matching-layer thickness for the lowest loss modes: r_1 = (*1*) 1.3278, (*2*) 1.525, (*3*) 1.8278 and (*4*) 9.0 μm. The vertical portions of the curves connect different roots of the dispersion equation at equal optical losses and are drawn as a guide to the eye to differentiate between fibres with different cores. The parameters of the periodic cladding are the same as in Fig. 3.

Note that, with increasing core radius, the range of allowed wave vector directions decreases. Varying the parameters of the intermediate layer, one can change the wave vector direction within the allowed range.

As pointed out by Abeeluck et al. [8], varying the pitch of the layered cladding may lead to two light propagation regimes, depending on wavelength. The long-wavelength transmission spectrum is determined by Bragg reflection from several high index/low index cladding layers. When the pitch exceeds the wavelength in vacuum, the spectral features of the structure can be understood in terms of an antiresonant model as the thickness of the structure increases further.

Studies concerned with antiresonance effects in Bragg fibres examined simultaneous variations in the thicknesses of all identical layers in a periodic cladding [8, 13, 17, 18]. The position of resonances was shown to be most sensitive to the high-index cladding layer adjacent to the core.

Varying the parameters of the adjacent layer at a fixed core diameter and fixed thicknesses of the layers in the periodic cladding also influences the optical properties of the fibre. For example, a linear decrease in the dimensions of the matching layer ($d_{\mathrm{M}} \gg \lambda_0$) along the fibre axis leads not only to periodic optical loss oscillations but also to periodic oscillations in light scattering by the lateral surface of the fibre [19].

Figure 6 shows the optical loss as a function of matching-layer thickness, d_{M}, for a Bragg fibre at $\lambda_0 = 1$ μm and different r_1 values. The optical loss (calculated according to the resultant curve ABCDEFGHI in Fig. 3b) is a periodic function of d_{M}. Both the lowest and highest loss values in each period are slightly lower than those in the preceding period. Moreover, the difference between the highest and lowest loss values decreases with increasing d_{M}.

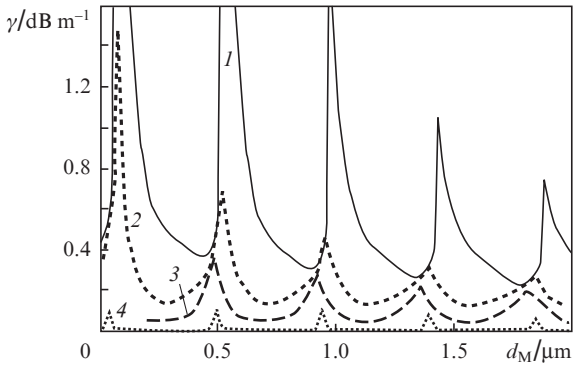

Figure 6. Optical loss as a function of matching-layer thickness at r_1 = (*1*) 1.3278, (*2*) 1.525, (*3*) 1.8278 and (*4*) 9.0 μm. The parameters of the periodic cladding are the same as in Fig. 3; $\lambda_0 = 1$ μm.

The resonance or antiresonance condition for the intermediate layer can be written in the form [13]

$$k_2 d_{\mathrm{M}} = \pi s, \tag{9}$$

where k_2 is the transverse wave vector component in the intermediate layer and s is an integer for resonances and a half-integer for antiresonances. For curve (*3*) (r_1 = 1.8278 μm), the optical loss is highest at d_{M} = 0.488, 0.926, 1.364 and 1.801 μm, with $\mathrm{Re}\,n_{\mathrm{eff}}$ = 0.988, 0.983, 0.980 and 0.977, respec-

tively. The changes in $\mathrm{Re}\,n_{\mathrm{eff}}$ lead to slight changes in k_2: 7006639.575, 7035515.209, 7052018.392 and 7068432.673 m^{-1}. Substituting these values into Eqn (9), we obtain s = 1.088, 2.074, 3.062 and 4.052. For the loss minima, we have s = 1.597, 2.596, 3.603 and 4.602.

The loss extrema in curve (*4*) (r_1 = 9.0 μm) correspond to s = 1.079, 1.587. 2.079, 2.587, 3.079, 3.588 and 4.072. Neglecting the slight variations in k_2 between neighbouring resonances, we obtain a spacing between them $\Delta d_{\mathrm{M}} = \pi/k_2$. For the average k_2 of an intermediate layer with r_1 = 1.8278 μm, the calculated spacing is Δd_{M} = 446.1 nm. According to Fig. 6, the average spacing between the loss maxima in curve (*3*) is 437.7 nm.

The above estimates lead us to conclude that the periodic variation of the optical loss with layer thickness is due to the resonances and antiresonances in the intermediate layer. The slight discrepancy between the above Δd_{M} values may arise from the following: (1) Bessel functions are not strictly periodic. (2) The spacing can be influenced by the resonances of the cladding as a whole and by those of the constituent layered resonators.

As shown earlier [19, 20], the periodic variation in optical loss due to variations in the thickness of the intermediate layer fits well with predictions of the antiresonant model. An antiresonance in the intermediate layer reduces the optical loss of radiation propagating through the core, while a resonance increases it. The above mode analysis clearly shows that the resonance condition corresponds to two-mode light propagation through the fibre, whereas the antiresonance condition, to single-mode light propagation (Fig. 3b).

In this study, major attention was paid to variations in the thickness of the intermediate layer, but variations in its refractive index give similar results. It is worth noting that antiresonance properties of the intermediate layer are more pronounced when its refractive index exceeds that of the layers in the periodic cladding.

5. Conclusions

We examined the mode composition of light and the optical loss of the modes in a hollow-core Bragg fibre with an intermediate layer between its core and periodic cladding. The optical characteristics of the fibre were calculated using the transfer matrix method. Numerical calculations for a Bragg fibre with a variable intermediate-layer thickness demonstrate that both single- and two-mode transmission regimes are possible. The major modes of the fibre are TE_{01} and TE_{02}. Any TE_{0k} mode of a standard Bragg fibre can be transformed into the fundamental mode of a Bragg fibre with an intermediate layer by varying the thickness of the intermediate layer. The intermediate-layer thicknesses that correspond to loss maxima and minima in the fibre and have been determined numerically using transfer matrices and in an antiresonance model agree well. Two-mode fibre excitation corresponds to a resonance in the intermediate layer, and the single-mode regime corresponds to an antiresonance.

References

1. Xu Y., Lee R.K., Yariv A. *Opt. Lett*., **25**, 1756 (2000).
2. Bassett I.M., Argyros A. *Opt. Express*, **10**, 1342 (2002).
3. Aleshkina S.S., Likhachev M.E., Uspenskii Yu.A., Bubnov M.M. *Kvantovaya Elektron*., **40**, 893 (2010) [*Quantum Electron*., **40**, 893 (2010)].
4. Likhachev M.E., Semjonov S.L., Bubnov M.M., et al. *Kvantovaya Elektron*., **36**, 581 (2006) [*Quantum Electron*., **36**, 581 (2006)].
5. Yeh P., Yariv A., Marom E.J. *J. Opt. Soc. Am*., **68**, 1196 (1978).
6. Martijn de Sterke C., Bassett I.M., Street A.G. *J. Appl. Phys*., **76**, 680 (1994).
7. Kawanishi T., Izutsu M. *Opt. Express*, **7**, 10 (2000).
8. Abeeluck A.K., Litchinitser N.M., et al. *Opt. Express*, **10**, 1320 (2002).
9. Argyros A. *Opt. Express*, **10**, 1411 (2002).
10. Guo Sh., Albin S., Rogowski R.S. *Opt. Express*, **12**, 198 (2004).
11. Mizrahi A., Schachter L. *Opt. Express*, **12**, 3156 (2004).
12. Sakai Jun-ichi, Nouchi P. *Opt. Commun*., **249**, 153 (2005).
13. Biryukov A.S., Bogdanovich D.V., Gaponov D.A., et al. *Kvantovaya Elektron*., **38**, 620 (2008) [*Quantum Electron*., **38**, 620 (2008)].
14. Chew W.C. *Waves and Fields in Inhomogeneous Media* (New York: Van Nostrand, 1990).
15. Kaliteevskii M.A., Nikolaev V.V., Abram R.A. *Opt. Spektrosk*., **88**, 871 (2000).
16. Jahnke E., Emde F., Losch F. *Tables of Higher Functions* (New York: McGraw-Hill, 1960; Moscow: Nauka, 1964).
17. Litchinitser N.M., Abeeluck A.K., Headley C. *Opt. Lett*., **27**, 1592 (2002).
18. Litchinitser N.M., Dunn S.C., Usner B., et al. *Opt. Express*, **11**, 1243 (2003).
19. Kulchin Yu.N., Zinin Yu.A., Nagornyi I.G., Voznesenskii S.S. *Opt. Spektrosk.*, **111**, 858 (2011).
20. Kul'chin Yu.N., Zinin Yu.A., Nagorny I.G. *Pis'ma Zh. Tekh. Fiz.*, **37**, 58 (2011).